Letter

Quantum metric induced phases in Moiré materials

Ahmed Abouelkomsan,* Kang Yang,* and Emil J. Bergholtz
Department of Physics, Stockholm University, AlbaNova University Center, 106 91 Stockholm, Sweden

(Received 24 February 2022; revised 1 November 2022; accepted 23 December 2022; published 10 February 2023)

We show that, quite generally, quantum geometry plays a major role in determining the low-energy physics in strongly correlated lattice models at fractional band fillings. We identify limits in which the Fubini-Study metric dictates the ground states and show that this is highly relevant for Moiré materials leading to symmetry breaking and interaction driven Fermi liquids. This phenomenology stems from a remarkable interplay between the quantum geometry and interaction which is absent in continuum Landau levels but generically present in lattice models where these terms tend to destabilize, e.g., fractional Chern insulators. We explain this as a consequence of the fundamental asymmetry between electrons and holes for band projected normal ordered interactions, as well as from the perspective of a self-consistent Hartree-Fock calculation. These basic insights about the role of the quantum metric, when dominant, turn an extremely strongly coupled problem into an effectively weakly coupled one, and may also serve as a guiding principle for designing material setups. We argue that this is a key ingredient for understanding symmetry-breaking phenomena recently observed in Moiré materials.

DOI: 10.1103/PhysRevResearch.5.L012015

I. INTRODUCTION

The application of geometry in physics continues to stimulate new fundamental insights. One of the most prominent examples is the general relativity. In condensed matter physics, the role of geometry has been in the limelight since the discovery of the geometric Berry phase [1,2], which is the phase accumulated during an adiabatic evolution. The Berry phase has proven to be critical to topological states and transport properties [3–14]. Quantum states also trace out a distance during an adiabatic evolution, which is captured by a metric [15,16]. The geometric concept of distance has been well recognized in quantum information theory [17–19], and it has also begun to attract interest in condensed matter physics [20–32]. Examples include the collective excitations of quantum Hall states [33–37] and bosonic phenomena such as superfluidity and Bose-Einstein condensation [38–41] in flat bands.

Flat, or nearly dispersionless, bands provide an ideal arena for strongly correlated states. The most prominent example thereof is the quantum Hall system exhibiting exactly flat bands in the continuum limit, and a rich phenomenology of strongly correlated states [42]. Flat bands of lattice models are known to in principle exhibit an even richer phenomenology [43–52], for which the recently engineered superlattice Moiré materials provide remarkably versatile flat-band structures [53–59] that can be controlled in experiments [60,61].

In this letter, we show that the Fubini-Study (FS) metric [15,16,62] has a profound impact on the low-energy physics of strongly interacting lattice models and that it can induce fermionic phases in lattice flat-band systems that have no direct analog in continuum Landau levels. We derive an emergent kinetic energy, which explicitly depends on the FS metric, through two distinct but mutually converging approaches: via a particle-hole (PH) transformation and a self-consistent Hartree-Fock calculation. While these results in principle have a wide range of applicability, here we focus on applying this to realistic Moiré systems for which we find that the quantum metric plays a preeminent role. Indeed, recent experiments have identified a large number of symmetry broken states [61,63–65]. Here, we provide an intuitive picture of the symmetry breaking: electrons (holes) tend to occupy regions of Brillouin zone (BZ) with short (long) quantum distances as quantified by a small (large) quantum metric. The main difference between this work and previous ones [9,20,21,55,57] about the quantum metric is that we do not seek analogs between flat bands and Landau levels at the single-particle level. The role of the quantum metric here purely comes from many-body interacting effects [66]. The quantum distance turns out to be vital in reducing a strongly interacting question to a weakly interacting question.

II. QUANTUM METRIC

In quantum physics, there is a natural notion of distance between quantum states by regarding them as normalized complex vectors [15,16,62,67]. In a tight-binding lattice model, the periodic part $\mu(\mathbf{k})$ of the Bloch states $\langle \mathbf{x}|\mathbf{k}\rangle = \exp(i\mathbf{k}\cdot\mathbf{x})\mu(\mathbf{k})$ is a vector of finite dimension. This gives rise

*These authors contributed equally to this work.

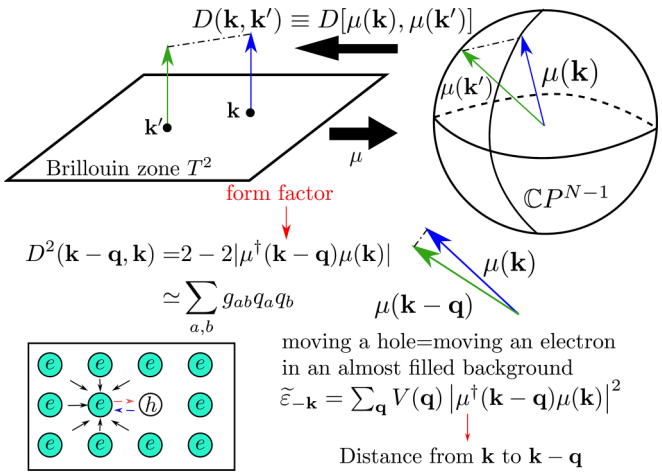

FIG. 1. Geometric interpretation of the form factor in band projections. The Bloch state $\mu(\mathbf{k})$ maps the Brillouin zone to a complex projective space $\mathbb{C}P^{N-1}$. The geometric information of the quantum states on $\mathbb{C}P^{N-1}$ can be pulled back to the Brillouin zone. The norm of the form factor directly reflects the quantum distance and the Fubini-Study metric. The exchange interaction $\tilde{\varepsilon}$ relies on the quantum distance and brings nontrivial hole dispersion.

to a distance measuring the difference between Bloch vectors at momenta $\mathbf{k}$ and $\mathbf{k}'$,

$$D^2(\mathbf{k},\mathbf{k}') = 2 - 2|\mu^\dagger(\mathbf{k})\mu(\mathbf{k}')|, \tag{1}$$

as illustrated in Fig. 1. Here $\mu^\dagger(\mathbf{k})\mu(\mathbf{k}')$ is the inner product $\sum_{j=1}^{N} \mu_j^*(\mathbf{k})\mu_j(\mathbf{k}')$ for a model with N bands. To gain some intuition, note that identical Bloch vectors at $\mathbf{k}$ and $\mathbf{k}'$ yield $D = 0$ while orthogonal ones give $D = \sqrt{2}$, consistent with Pythagoras' theorem.

At small separation $\mathbf{q}$, this distance leads to a FS metric $g_{ab}(\mathbf{k})$:

$$D^2(\mathbf{k}-\mathbf{q},\mathbf{k}) \approx \sum_{a,b=1}^{2} g_{ab}(\mathbf{k}) q_a q_b. \tag{2}$$

Equivalently, the FS metric can be expressed as [20,68]

$$2g_{ab}(\mathbf{k}) = \partial_a\mu^\dagger(\mathbf{k})\partial_b\mu(\mathbf{k}) - [\partial_a\mu^\dagger(\mathbf{k})\mu(\mathbf{k})][\mu^\dagger(\mathbf{k})\partial_b\mu(\mathbf{k})] + (a \leftrightarrow b). \tag{3}$$

One may note that the distance (1) is different from the geodesic distance [16] or the Hilbert–Schmidt quantum distance [17,23], but all these definitions coincide when the quantum distance is small, leading to the same effective metric. Mathematically the terminology of distance and metric tensor [69] introduced here may need careful treatment. More details can be found in the Supplemental Material (SM) [70].

III. EMERGENT KINETIC ENERGY

In a flat-band model the relevant physics is given by the projected interaction of electrons:

$$H = \frac{1}{2}\sum_{\mathbf{q},\mathbf{k},\mathbf{k}'} V(\mathbf{q})[\mu^\dagger(\mathbf{k}-\mathbf{q})\mu(\mathbf{k})][\mu^\dagger(\mathbf{k}'+\mathbf{q})\mu(\mathbf{k}')] \times c^\dagger_{\mathbf{k}-\mathbf{q}} c^\dagger_{\mathbf{k}'+\mathbf{q}} c_{\mathbf{k}'} c_{\mathbf{k}}. \tag{4}$$

The key ingredient is the projected density operator at momentum $\mathbf{q}$, which is the product of the operators $c^\dagger_{\mathbf{k}-\mathbf{q}} c_{\mathbf{k}}$ and the form factor $\mu^\dagger(\mathbf{k}-\mathbf{q})\mu(\mathbf{k})$. We consider a single band, i.e, we freeze any additional degrees of freedom such as the spin and the valley. As there is no kinetic energy, the electrons are strongly interacting and the many-body state seems to be very complicated. Previous work [66,71] notices that under a PH transformation the Fermi liquid may be a good candidate for ground states. At first glance, however, the Hamiltonian seems PH symmetric. The enigma lies in the fluctuating band geometry and the correlated nature of hole-like degrees of freedom. A PH transformation maps $c_{\mathbf{k}} \to d^\dagger_{-\mathbf{k}}$. In addition to the transformation on operators, we also need to transform the concomitant reference state, from the vacuum of electrons $|\Omega\rangle$ to the vacuum of holes $|\Omega'\rangle = \prod_{\mathbf{k}} c^\dagger_{\mathbf{k}}|\Omega\rangle$. The low-energy excitations of $|\Omega'\rangle$ are described by creating a few holes. To better capture this physical process, we need to normal order the Hamiltonian by moving all hole creation operators to the right of hole annihilation operators. This procedure gives the following Hamiltonian:

$$\bar{\bar{H}} = \sum_{\mathbf{k}} \varepsilon_{\mathbf{k}} d^\dagger_{\mathbf{k}} d_{\mathbf{k}} + \frac{1}{2}\sum_{\mathbf{q},\mathbf{k},\mathbf{k}'} V(\mathbf{q})[\mu^\dagger(-\mathbf{k})\mu(\mathbf{q}-\mathbf{k})] \times [\mu^\dagger(-\mathbf{k}')\mu(-\mathbf{k}'-\mathbf{q})] d^\dagger_{\mathbf{k}-\mathbf{q}} d^\dagger_{\mathbf{k}'+\mathbf{q}} d_{\mathbf{k}'} d_{\mathbf{k}}. \tag{5}$$

Apart from a similar interaction term to electrons, holes receive a quadratic term that is generically dispersing (an exception is Landau levels where it is constant) [66]. This term reflects the fact that the kinetics of a hole is described by how an electron moves in an electron background (see Fig. 1). It can be decomposed into two parts: $\varepsilon = \bar{\varepsilon} + \tilde{\varepsilon}$. The first constant term comes from a uniform background repulsion and is equivalent to a chemical potential (details in the SM [70]). The second term is nontrivial, resulting from the exchange interaction, $\tilde{\varepsilon}_{-\mathbf{k}} = \sum_{\mathbf{q}} V(\mathbf{q})|\mu^\dagger(\mathbf{k}-\mathbf{q})\mu(\mathbf{k})|^2$, where the form factor norm enters.

A key observation is that the form factor norm occurring in $\tilde{\varepsilon}_{-\mathbf{k}}$ describes the distance between two Bloch states $\mu(\mathbf{k})$ and $\mu(\mathbf{k}-\mathbf{q})$. The exchange interaction is thus jointly determined by the *interaction potential* and the *quantum distance*. The kinetic energy of holes is dispersing as long as the quantum geometry pulled back to the BZ is not uniform. For small momentum $\mathbf{q}$, $\tilde{\varepsilon}_{-\mathbf{k}}$ can be expanded by the FS metric $|\mu^\dagger(\mathbf{k}-\mathbf{q})\mu(\mathbf{k})|^2 \simeq 1 - \sum_{ab} q_a q_b g_{ab}(\mathbf{k})$:

$$\tilde{\varepsilon}_{-\mathbf{k}} \simeq \sum_{\mathbf{q}} V(\mathbf{q}) e^{-\sum_{ab} q_a q_b g_{ab}(\mathbf{k})}, \tag{6}$$

where we further approximate the parabolic expansion by lifting it to the exponent so that the norm is still positive at large $\mathbf{q}$. This ansatz of form factors also appears in the context of ideal fractional Chern insulators (FCI) [20], although the focus here is on the opposite aspects, namely, the qualitative deviations from Landau level physics.

Intuitively, one may expect that the hole dispersion and the Fermi-liquid idea would only be useful at high electronic band filling. Remarkably, however, the Fermi liquid prevails in a wide range of fillings ν [71] for Moiré systems. This can be understood from a self-consistent picture of Landau's Fermi

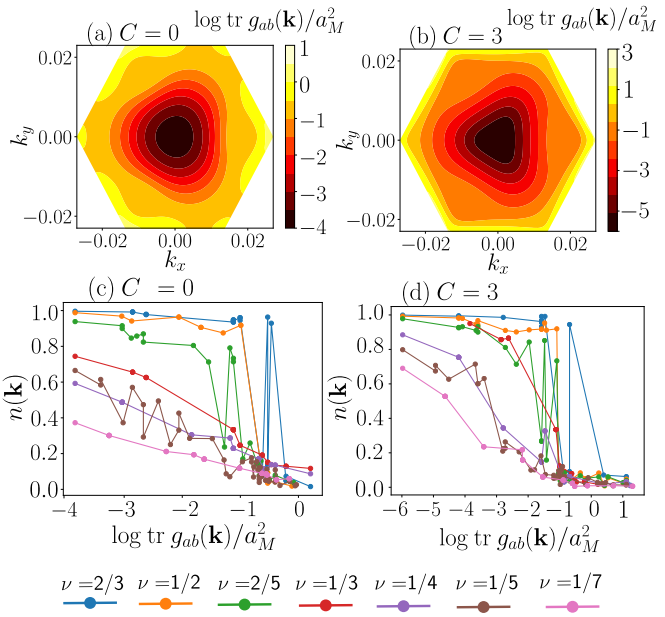

FIG. 2. Metric-induced phases in TLG-hBN $C = 0$ valence band and $C = 3$ valence band obtained by switching the sign of the gate-voltage: (a and b) Contour plots of log tr $g_{ab}(\mathbf{k})/a_M^2$, where a_M is the Moiré unit cell lattice constant. (c and d) Lowest energy ground state electron occupation $n(\mathbf{k}) = \langle c_{\mathbf{k}}^\dagger c_{\mathbf{k}}\rangle$ obtained from exact diagonalization [70] vs log tr $g_{ab}(\mathbf{k})/a_M^2$ as a function of electron band filling ν. We use gate voltage $U = \pm 0.02$ eV [72].

liquids, yielding a Fock energy induced by the interaction [70]

$$E_{\mathbf{k}} \simeq -\sum_{\mathbf{q}} V(\mathbf{q}) e^{-\sum_{ab} q_a q_b g_{ab}(\mathbf{k})} \langle c_{\mathbf{k}-\mathbf{q}}^\dagger c_{\mathbf{k}-\mathbf{q}}\rangle. \tag{7}$$

Because of the nonuniform geometry, electrons prefer to fill the areas in the BZ with small tr g (Fig. 2), where they can benefit from a lower Fock energy due to the smaller quantum distance. This renders the Fermi liquid a natural ground-state candidate also in the electron picture. The hole dispersion can be regarded as the extreme case when the band is completely filled ($\langle c_{\mathbf{k}}^\dagger c_{\mathbf{k}}\rangle = 1$ for all $\mathbf{k}$). As we will show, Moiré systems have rapidly decaying form factors. Then the partial summation (7) over the electron-filled region is not very different from the whole BZ summation (6). So, the hole energy gives a good estimate of the self-consistent Hartree-Fock Hamiltonian of the electrons, $E_{\mathbf{k}} \simeq -\tilde{\varepsilon}_{-\mathbf{k}}$, where the minus signs come from the PH relation. Explicit comparisons can be found in the SM [70].

Equations (6) and (7) and their relevance to Moiré materials are the main results of this letter. The nonuniform quantum geometry and the finite electron density induce a nontrivial emergent kinetic energy in flat bands. Locally, such a nonuniform geometry is captured by the FS metric and the kinetic energy can be obtained by integrating the interaction potential with the metric. This emergent kinetic energy naturally appears in the hole Hamiltonian, as hole degrees of freedom have the completely filled band as a reference state. In contrast, Landau levels have an exactly flat geometric structure and the Hamiltonian (any band projected translation invariant two-body interaction) is always PH symmetric.

IV. METRIC-DOMINATED CONDITIONS

We expect that Eq. (6) gives the dominant contribution to the emergent kinetic energy when the product of the interaction potential and the form factor decays fast enough in $\mathbf{q}$. The form factor reflects the quantum distance. As the BZ is fixed to be two-dimensional (2D), we can envisage its image $\mu(\mathbf{k})$ to be some 2D subspace of the complex projective space $\mathbb{C}P^{N-1}$. The average distance between $\mu(\mathbf{k}-\mathbf{q})$ and $\mu(\mathbf{k})$ thus depends on to which extent this subspace extends in $\mathbb{C}P^{N-1}$. A natural condition is that N should be large, otherwise most states in $\mathbb{C}P^{N-1}$ are nearby. Especially for a topologically non-trivial band, the image of the BZ tends to span much of $\mathbb{C}P^{N-1}$. Thus a system with sufficient many bands is likely to support a fast-decaying form factor. An excellent approximation is obtained by considering the finite thickness of the 2D material. This results in a potential decaying in the momentum space, for example, the Zhang-Das Sarma potential $V(\mathbf{q}) = 2\pi e^2 \exp(-lq)/q$, where l is the sample thickness [73].

V. APPLICATIONS TO MOIRÉ MATERIALS

The number of minibands in Moiré systems is estimated as $N \simeq (|\mathbf{Q}_0|/|\mathbf{G}_0|)^2 \sim 10^3$, where $\mathbf{G}_0$ is the primitive Moiré reciprocal lattice vector and $\mathbf{Q}_0$ is the primitive reciprocal lattice vector of the original lattice. So Moiré materials satisfy the condition of sufficiently many bands. In continuum approximations, the Moiré Bloch states $|\psi_{\mathbf{k}}\rangle$ are constructed by superposing the original Bloch states $|\mathbf{k}+\mathbf{G}\rangle$ differed by Moiré reciprocal wave vectors, $|\psi_{\mathbf{k}}\rangle = \sum_{\mathbf{G}} \mu(\mathbf{k},\mathbf{G})|\mathbf{k}+\mathbf{G}\rangle$. Here we omit other indices for spins or valleys. The form factor is obtained as $\sum_{\mathbf{G}} \mu^*(\mathbf{k}-\mathbf{q},\mathbf{G})\mu(\mathbf{k},\mathbf{G})$. A natural definition of Moiré Bloch vectors is given by $\mu(\mathbf{k},\mathbf{G})$ with $\mathbf{G}$ as an index of components. We show in the SM [70] that the Moiré form factors are indeed quickly decaying.

Different from conventional tight-binding models, the norm of the Moiré form factor is not periodic in $\mathbf{q}$. A usual Bloch vector $\mu(\mathbf{k})$ and its BZ translated counterpart $\mu(\mathbf{k}+\mathbf{Q})$ only differs by a phase $\phi_{\mathbf{k},\mathbf{Q}}$. In contrast, the Moiré BZ translated pairs are different by an additional cyclic transformation on its components $\mu(\mathbf{k}+\mathbf{G}',\mathbf{G}) = \exp(i\phi_{\mathbf{k},\mathbf{G}'})\mu(\mathbf{k},\mathbf{G}+\mathbf{G}')$. For this reason, even the contribution $\bar{\varepsilon}_{\mathbf{k}}$ is (weakly) dispersing and $\tilde{\varepsilon}_{\mathbf{k}}$ becomes more complicated [70]. However, all of these differences are happening at momenta equal or larger than $\mathbf{G}_0$ and since the Moiré form factors are quickly decaying, these modifications are minimal. Hence (6) remains accurate. Equipped with the connection between the FS metric and an emergent dispersion, we proceed to analyze possible phases in prominent Moiré systems such as trilayer graphene and twisted bilayer graphene, both aligned with hexagonal boron nitride. Both these two setups and several other related ones have attracted ample interest as tunable platforms for studying strongly correlated phases such as correlated insulators and superconductivity [63,76–95].

VI. TRILAYER GRAPHENE ALIGNED WITH BORON-NITRIDE

The Moiré system trilayer graphene aligned with hBN hosts a nearly flat valence band below charge neutrality upon applying a gate voltage across the layers [72,96]. At the

noninteracting level, neglecting possible strain effects [97], the flat band could be topologically trivial with Chern number $C = 0$ or topologically nontrivial with $C = 3$, depending on the sign of the applied gate voltage. It was theoretically shown [71] that this system could host Fermi liquid phases dictated by the single-hole dispersion for a wide range of filling. Remarkably, the emergent dispersion greatly influences the average electron occupation down to very low fillings. Regardless of the value of the Chern number, the trilayer graphene aligned with boron-nitride (TLG-hBN) valence band has a nontrivial and far from flat FS metric quantified by the trace tr $g(\mathbf{k})$ shown in Figs. 2(a) and 2(b). We find the electron occupation in momentum space $n(\mathbf{k})$ to correlate well with log tr $g(\mathbf{k})/a_M^2$, as indicated in Figs. 2(c) and 2(d) for representative filling fractions $\nu \leqslant 2/3$. This shows that the origin of such a correlation is mainly induced by the highly fluctuating FS metric that results in a kinetic energy with large bandwidth. As shown in Figs. 2(a) and 2(b), we find log tr $g(\mathbf{k})/a_M^2$ to share the same qualitative features with the hole dispersion [71] up to very high electron fillings, where it starts to deviate from the hole energy. The gradual disappearance of well-defined Fermi surfaces, manifested in the sharp jumps in the occupation $n(\mathbf{k})$ as shown in Figs. 2(c) and 2(d), as the electron filling ν decreases signals possible transitions from the Fermi liquid state to competing states. Charge density waves (CDW) are natural candidates at fillings that are commensurate with the triangular Moiré lattice. To illustrate this, we provide numerical evidence for a possible CDW at $\nu = 1/3$ for the $C = 0$ band through the threefold ground state degeneracy shown in Fig. 3(a) and the static structure factor peaks shown in Fig. 3(b). The effects of quantum geometry are, however, present even when there is an absence of a well-defined Fermi surface. Although the sharp Fermi surface is blurred [cf. $\nu = 1/3$ in Fig. 2(c)], the ground state occupation correlates well with tr g as the electrons tend to stay in regions with small tr g. Moreover, the nonuniform quantum metric reflects a strong PH asymmetry; we find no evidence of CDW at the PH dual filling $\nu = 2/3$, as illustrated in Figs. 3(c) and 3(d). Indeed, the occupation $n(\mathbf{k})$ [cf. $\nu = 2/3$ in Fig. 2(c)], when averaged over a number of low-lying energy states, shows clear signs of a Fermi liquid state [70]. This asymmetry may be attributed to the different Fermi-surface geometries corresponding to $\nu = 1/3$ and $\nu = 2/3$, dictated by the FS metric. The systematic identification of the ground states at different commensurate fillings and the nature of transitions provides avenues for future work starting from the insights presented here, including the study of possible instabilities starting from Fermi surfaces suggested by the FS metric.

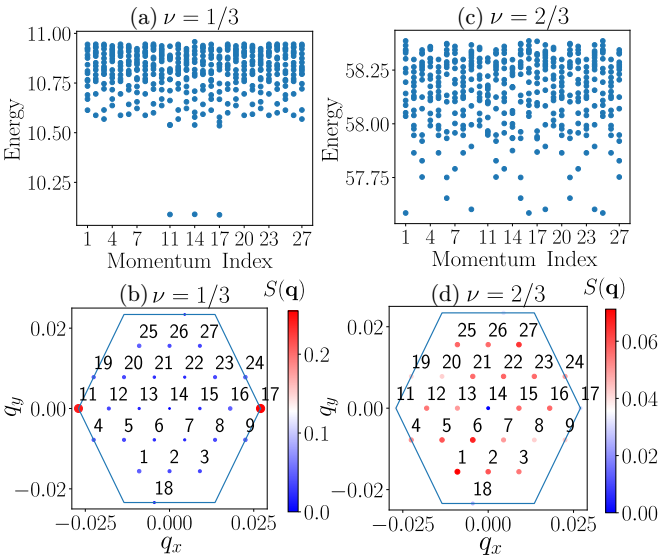

FIG. 3. Particle-hole asymmetry in TLG-hBN $C = 0$ valence band: (a and b) Evidence of charge density wave at $\nu = 1/3$. (a) Many-body spectrum showing threefold degeneracy at three different momenta corresponding to the three possible charge configurations when the unit-cell is tripled. (b) The projected static structure constant calculated in the lowest energy ground state $S(\mathbf{q}) = \langle \hat{\rho}_{\mathbf{q}}^{\text{proj}} \hat{\rho}_{-\mathbf{q}}^{\text{proj}} \rangle$ with $\hat{\rho}_{\mathbf{q}}^{\text{proj}} = \sum_{\mathbf{k}} \mu^\dagger(\mathbf{k}-\mathbf{q})\mu(\mathbf{k}) c_{\mathbf{k}-\mathbf{q}}^\dagger c_{\mathbf{k}}$. Prominent peaks are observed at the **K** points. (c and d) Absence of charge density wave at $\nu = 2/3$. (c) Many-body spectrum with no clear separated low-energy sector. (d) Featureless static structure factor $S(\mathbf{q})$ with no prominent peaks.

VII. TWISTED BILAYER GRAPHENE ALIGNED WITH BORON-NITRIDE

Next we study twisted bilayer graphene aligned with boron-nitride (TBG-hBN). The alignment with hBN gaps out the flat bands of twisted bilayer graphene and makes them acquire a nonzero Chern number $C = \pm 1$ [74,98]. Earlier theoretical studies [57,71,99] have predicted the possibility of realizing zero magnetic field FCI state at fractional fillings of the flat bands of TBG-hBN. These FCI states compete with possible CDW at commensurate fillings [100]. Such competition depends on the relaxation ratio $r = w_0/w_1$, where w_0 and w_1 are the interlayer tunneling strengths at the AA-stacked and AB-stacked regions, respectively. Assuming spin and valley polarization, we focus on the valence band at filling fraction $\nu = 1/3$ and vary r. (Qualitatively similar results were obtained in the valence band at $\nu = 2/3$ and in the conduction band at both $\nu = 1/3$ and $\nu = 2/3$.) As the value of r increases, FS metric fluctuations become more prominent and a transition from FCI to CDW occurs (Fig. 4). The critical value of r of such a transition is sensitive to the model parameters such as w_1 and twist angle θ [14]. Recent experiments [61] have confirmed the existence of FCI states in TBG, albeit with the application of a weak magnetic field. It was argued [14,61] that the role of the weak magnetic field, similar to a smaller r, is to make the Berry curvature more uniform, thus stabilizing the zero-field FCI. Note that in this system, the FS metric fluctuates in sync with the Berry curvature [14,55,57], and the magnetic field or the ratio r also flattens the FS metric. As a consequence, we here provide a complementary interpretation of the competition between FCI and CDW based on the FS metric. FCI prefer the electron density to be uniform in momentum space and the Berry curvature, the effective "magnetic field," to be nonvanishing in these regions. If the metric is uniform, electrons do not have priorities in the BZ and this condition can be satisfied. As the ratio r increases, however, the FS metric becomes less uniform as shown Figs. 4(a)–4(c). Accordingly, there is a tendency for the electrons to occupy states with lower tr $g(\mathbf{k})$ to minimize

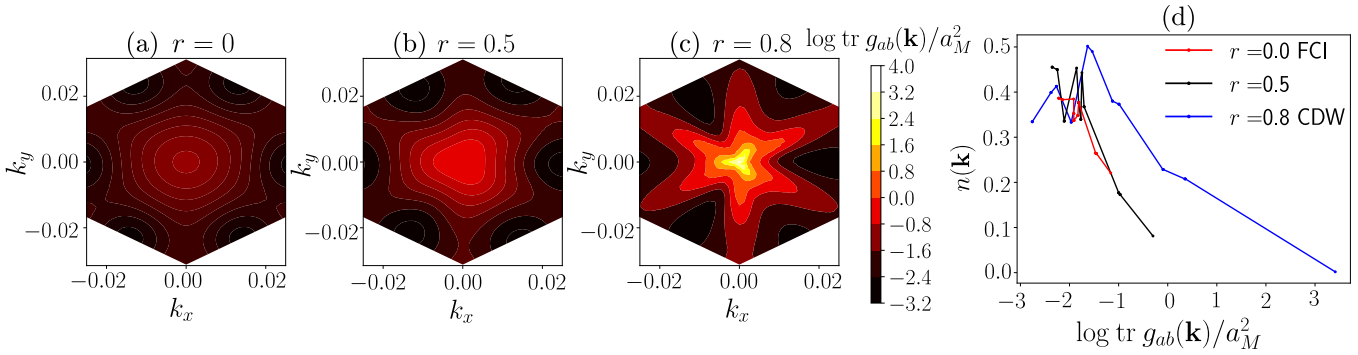

FIG. 4. Fubini-Study metric effect in the spin and valley polarized $C = 1$ valence band in TBG-hBN: (a)–(c) Contour plots of $\log \mathrm{tr}\, g_{ab}(\mathbf{k})/a_M^2$ at twist angle $\theta = 1.05^\circ$ and mass term [74] $M = 15$ meV for different values of $r = w_0/w_1$. a_M is the Moiré unit cell lattice constant. (d) Lowest energy ground state electron occupation $n(\mathbf{k}) = \langle c_{\mathbf{k}}^\dagger c_{\mathbf{k}} \rangle$ obtained from exact diagonalization [70] at $\nu = 1/3$ vs $\log \mathrm{tr}\, g_{ab}(\mathbf{k})/a_M^2$ for different values of r. The criteria for FCI agree with counting rules in Ref. [75].

the Fock energy according to Eqs. (5)–(7). This leads to a varying $n(\mathbf{k})$, destabilizing the FCI state since it is a liquid of roughly uniform density. This is highlighted in Fig. 4(d), where we show how the occupation $n(\mathbf{k})$ evolves for different values of r as a function of $\log \mathrm{tr}\, g(\mathbf{k})/a_M^2$.

VIII. DISCUSSION

We have shown that the quantum geometry in terms of the Fubini-Study metric explicitly appears in the effective Hamiltonian description of strongly interacting electrons in a flat band, yielding an emergent kinetic energy stemming from the collective interactions. This suggests a generic and physically intuitive picture of symmetry breaking states—and their microscopic provenance—which have been observed in recent experiments on Moiré materials [61,63–65].

Our theory also provides an alternative criterion for the stability of FCI. Whereas previous studies [8,20,101] were based on the similarity of the density algebra to quantum Hall effects, here we give a microscopic interpretation of band geometry. The uniformity of the Fubini-Study metric dictates where the electrons are likely to condensate in momentum space. The observed FCI/CDW transitions in Ref. [61] may also be explained by the more uniform metric tuned through the magnetic field or interlayer interaction ratio w_0/w_1. As a comparison, the interpretation of the Berry curvature from a microscopic view is less clear [12].

The paramount role of the Fubini-Study metric in fractionally filled Moiré bands may serve as a guiding principle in materials design aiming to realize various exotic phases. Moreover, it effectively turns experimentally relevant instances of an extremely strongly interacting problem into an effectively weakly interacting one, thus enabling the use of standard techniques of theoretical physics.

ACKNOWLEDGMENTS

We acknowledge helpful discussions with Yonglong Xie, Shaowen Chen, Zhao Liu, Ipsita Mandal, and Daniel Varjas. The authors are supported by the Swedish Research Council (VR, Grant No. 2018-00313), the Wallenberg Academy Fellows program of the Knut and Alice Wallenberg Foundation (No. 2018.0460), and the Göran Gustafsson Foundation for Research in Natural Sciences and Medicine.

[1] M. V. Berry, Quantal phase factors accompanying adiabatic changes, Proc. R. Soc. London A **392**, 45 (1984).
[2] D. N. Page, Geometrical description of Berry's phase, Phys. Rev. A **36**, 3479 (1987).
[3] M. Kohmoto, Topological invariant and the quantization of the hall conductance, Ann. Phys. **160**, 343 (1985).
[4] F. D. M. Haldane, Berry Curvature on the Fermi Surface: Anomalous Hall Effect as a Topological Fermi-Liquid Property, Phys. Rev. Lett. **93**, 206602 (2004).
[5] A. Stern, F. von Oppen, and E. Mariani, Geometric phases and quantum entanglement as building blocks for non-Abelian quasiparticle statistics, Phys. Rev. B **70**, 205338 (2004).
[6] D. Xiao, M.-C. Chang, and Q. Niu, Berry phase effects on electronic properties, Rev. Mod. Phys. **82**, 1959 (2010).
[7] M. Goerbig, From fractional Chern insulators to a fractional quantum spin Hall effect, Eur. Phys. J. B **85**, 15 (2012).
[8] S. A. Parameswaran, R. Roy, and S. L. Sondhi, Fractional Chern insulators and the W_∞ algebra, Phys. Rev. B **85**, 241308(R) (2012).
[9] T. S. Jackson, G. Möller, and R. Roy, Geometric stability of topological lattice phases, Nat. Commun. **6**, 8629 (2015).
[10] B. Yan and C. Felser, Topological materials: Weyl semimetals, Annu. Rev. Condens. Matter Phys. **8**, 337 (2017).
[11] B. Douçot, R. Danneau, K. Yang, J.-G. Caputo, and R. Mélin, Berry phase in superconducting multiterminal quantum dots, Phys. Rev. B **101**, 035411 (2020).
[12] D. Varjas, A. Abouelkomsan, K. Yang, and E. J. Bergholtz, Topological lattice models with constant Berry curvature, SciPost Phys. **12**, 118 (2022).
[13] S. H. Simon and M. S. Rudner, Contrasting lattice geometry dependent versus independent quantities: Ramifications for Berry curvature, energy gaps, and dynamics, Phys. Rev. B **102**, 165148 (2020).

[14] D. Parker, P. Ledwith, E. Khalaf, T. Soejima, J. Hauschild, Y. Xie, A. Pierce, M. P. Zaletel, A. Yacoby, and A. Vishwanath, Field-tuned and zero-field fractional Chern insulators in magic angle graphene, arXiv:2112.13837.

[15] J. Provost and G. Vallee, Riemannian structure on manifolds of quantum states, Commun. Math. Phys. **76**, 289 (1980).

[16] J. Anandan and Y. Aharonov, Geometry of Quantum Evolution, Phys. Rev. Lett. **65**, 1697 (1990).

[17] V. Bužek and M. Hillery, Quantum copying: Beyond the no-cloning theorem, Phys. Rev. A **54**, 1844 (1996).

[18] V. Vedral, M. B. Plenio, M. A. Rippin, and P. L. Knight, Quantifying Entanglement, Phys. Rev. Lett. **78**, 2275 (1997).

[19] T. Baumgratz, M. Cramer, and M. B. Plenio, Quantifying Coherence, Phys. Rev. Lett. **113**, 140401 (2014).

[20] R. Roy, Band geometry of fractional topological insulators, Phys. Rev. B **90**, 165139 (2014).

[21] M. Claassen, C. H. Lee, R. Thomale, X.-L. Qi, and T. P. Devereaux, Position-Momentum Duality and Fractional Quantum Hall Effect in Chern Insulators, Phys. Rev. Lett. **114**, 236802 (2015).

[22] F. Piéchon, A. Raoux, J.-N. Fuchs, and G. Montambaux, Geometric orbital susceptibility: Quantum metric without Berry curvature, Phys. Rev. B **94**, 134423 (2016).

[23] J.-W. Rhim, K. Kim, and B.-J. Yang, Quantum distance and anomalous Landau levels of flat bands, Nature (London) **584**, 59 (2020).

[24] B. Mera and T. Ozawa, Engineering geometrically flat Chern bands with Fubini-Study Kähler structure, Phys. Rev. B **104**, 115160 (2021).

[25] Kristian Hauser A. Villegas and B. Yang, Anomalous Higgs oscillations mediated by Berry curvature and quantum metric, Phys. Rev. B **104**, L180502 (2021).

[26] F. Wu and S. Das Sarma, Quantum geometry and stability of Moiré flatband ferromagnetism, Phys. Rev. B **102**, 165118 (2020).

[27] J. Mitscherling and T. Holder, Bound on resistivity in flat-band materials due to the quantum metric, Phys. Rev. B **105**, 085154 (2022).

[28] C. Northe, G. Palumbo, J. Sturm, C. Tutschku, and E. M. Hankiewicz, Interplay of band geometry and topology in ideal Chern insulators in presence of external electromagnetic fields, Phys. Rev. B **105**, 155410 (2022).

[29] T. Ozawa and N. Goldman, Extracting the quantum metric tensor through periodic driving, Phys. Rev. B **97**, 201117(R) (2018).

[30] T. Ozawa and N. Goldman, Probing localization and quantum geometry by spectroscopy, Phys. Rev. Res. **1**, 032019(R) (2019).

[31] X. Tan, D.-W. Zhang, Z. Yang, J. Chu, Y.-Q. Zhu, D. Li, X. Yang, S. Song, Z. Han, Z. Li, Y. Dong, H.-F. Yu, H. Yan, S.-L. Zhu, and Y. Yu, Experimental Measurement of the Quantum Metric Tensor and Related Topological Phase Transition with a Superconducting Qubit, Phys. Rev. Lett. **122**, 210401 (2019).

[32] M. Yu, P. Yang, M. Gong, Q. Cao, Q. Lu, H. Liu, S. Zhang, M. B. Plenio, F. Jelezko, T. Ozawa, N. Goldman, and J. Cai, Experimental measurement of the quantum geometric tensor using coupled qubits in diamond, Natl. Sci. Rev. **7**, 254 (2019).

[33] F. D. M. Haldane, Geometrical Description of the Fractional Quantum Hall Effect, Phys. Rev. Lett. **107**, 116801 (2011).

[34] A. Gromov and D. T. Son, Bimetric Theory of Fractional Quantum Hall States, Phys. Rev. X **7**, 041032 (2017).

[35] S.-F. Liou, F. D. M. Haldane, K. Yang, and E. H. Rezayi, Chiral Gravitons in Fractional Quantum Hall Liquids, Phys. Rev. Lett. **123**, 146801 (2019).

[36] K. Yang, M. O. Goerbig, and B. Douçot, Collective excitations of quantum Hall states under tilted magnetic field, Phys. Rev. B **102**, 045145 (2020).

[37] Z. Liu, A. C. Balram, Z. Papić, and A. Gromov, Quench Dynamics of Collective Modes in Fractional Quantum Hall Bilayers, Phys. Rev. Lett. **126**, 076604 (2021).

[38] S. Peotta and P. Törmä, Superfluidity in topologically nontrivial flat bands, Nat. Commun. **6**, 8944 (2015).

[39] A. Julku, G. M. Bruun, and P. Törmä, Quantum Geometry and Flat Band Bose-Einstein Condensation, Phys. Rev. Lett. **127**, 170404 (2021).

[40] P. Törmä, S. Peotta, and B. A. Bernevig, Superfluidity and quantum geometry in twisted multilayer systems, arXiv:2111.00807.

[41] Y. Guan, O. V. Yazyev, and A. Kruchkov, Re-entrant magic-angle phenomena in twisted bilayer graphene in integer magnetic fluxes, Phys. Rev. B **106**, L121115 (2022).

[42] T. H. Hansson, M. Hermanns, S. H. Simon, and S. F. Viefers, Quantum H physics: Hierarchies and conformal field theory techniques, Rev. Mod. Phys. **89**, 025005 (2017).

[43] A. Kol and N. Read, Fractional quantum Hall effect in a periodic potential, Phys. Rev. B **48**, 8890 (1993).

[44] D. Sheng, Z.-C. Gu, K. Sun, and L. Sheng, Fractional quantum Hall effect in the absence of Landau levels, Nat. Commun. **2**, 389 (2011).

[45] N. Regnault and B. A. Bernevig, Fractional Chern Insulator, Phys. Rev. X **1**, 021014 (2011).

[46] Y.-F. Wang, H. Yao, C.-D. Gong, and D. N. Sheng, Fractional quantum Hall effect in topological flat bands with Chern number two, Phys. Rev. B **86**, 201101(R) (2012).

[47] Z. Liu, E. J. Bergholtz, H. Fan, and A. M. Läuchli, Fractional Chern Insulators in Topological Flat Bands with Higher Chern Number, Phys. Rev. Lett. **109**, 186805 (2012).

[48] S. Yang, Z.-C. Gu, K. Sun, and S. Das Sarma, Topological flat band models with arbitrary Chern numbers, Phys. Rev. B **86**, 241112(R) (2012).

[49] M. Trescher and E. J. Bergholtz, Flat bands with higher Chern number in pyrochlore slabs, Phys. Rev. B **86**, 241111(R) (2012).

[50] T. Liu, C. Repellin, B. A. Bernevig, and N. Regnault, Fractional Chern insulators beyond Laughlin states, Phys. Rev. B **87**, 205136 (2013).

[51] A. Sterdyniak, C. Repellin, B. A. Bernevig, and N. Regnault, Series of Abelian and non-Abelian states in $c > 1$ fractional Chern insulators, Phys. Rev. B **87**, 205137 (2013).

[52] E. J. Bergholtz and Z. Liu, Topological flat band models and fractional Chern insulators, Int. J. Mod. Phys. B **27**, 1330017 (2013).

[53] R. Bistritzer and A. H. MacDonald, Moiré bands in twisted double-layer graphene, Proc. Natl. Acad. Sci. USA **108**, 12233 (2011).

[54] E. Y. Andrei and A. H. MacDonald, Graphene bilayers with a twist, Nat. Mater. **19**, 1265 (2020).

[55] J. Wang, J. Cano, A. J. Millis, Z. Liu, and B. Yang, Exact Landau Level Description of Geometry and Interaction in a Flatband, Phys. Rev. Lett. **127**, 246403 (2021).

[56] J. Wang and Z. Liu, Hierarchy of Ideal Flatbands in Chiral Twisted Multilayer Graphene Models, Phys. Rev. Lett. **128**, 176403 (2022).

[57] P. J. Ledwith, G. Tarnopolsky, E. Khalaf, and A. Vishwanath, Fractional Chern insulator states in twisted bilayer graphene: An analytical approach, Phys. Rev. Res. **2**, 023237 (2020).

[58] G. Tarnopolsky, A. J. Kruchkov, and A. Vishwanath, Origin of Magic Angles in Twisted Bilayer Graphene, Phys. Rev. Lett. **122**, 106405 (2019).

[59] J. L. Lado and P. Liljeroth, Designer quantum matter in van der Waals heterostructures, arXiv:2102.11779.

[60] L. Balents, C. R. Dean, D. K. Efetov, and A. F. Young, Superconductivity and strong correlations in Moiré flat bands, Nat. Phys. **16**, 725 (2020).

[61] Y. Xie, A. T. Pierce, J. M. Park, D. E. Parker, E. Khalaf, P. Ledwith, Y. Cao, S. H. Lee, S. Chen, P. R. Forrester *et al.*, Fractional Chern insulators in magic-angle twisted bilayer graphene, Nature (London) **600**, 439 (2021).

[62] S. Kobayashi and K. Nomizu, *Foundations of Differential Geometry, 2 Volume Set*, Wiley Classics Library (Wiley, New York, 2009).

[63] A. T. Pierce, Y. Xie, J. M. Park, E. Khalaf, S. H. Lee, Y. Cao, D. E. Parker, P. R. Forrester, S. Chen, K. Watanabe, T. Taniguchi, A. Vishwanath, P. Jarillo-Herrero, and A. Yacoby, Unconventional sequence of correlated Chern insulators in magic-angle twisted bilayer graphene, Nat. Phys. **17**, 1210 (2021).

[64] H. Polshyn, Y. Zhang, M. A. Kumar, T. Soejima, P. Ledwith, K. Watanabe, T. Taniguchi, A. Vishwanath, M. P. Zaletel, and A. F. Young, Topological charge density waves at half-integer filling of a Moiré superlattice, Nat. Phys. **18**, 42 (2022).

[65] S. Bhowmik, B. Ghawri, N. Leconte, S. Appalakondaiah, M. Pandey, P. S. Mahapatra, D. Lee, K. Watanabe, T. Taniguchi, J. Jung *et al.*, Broken-symmetry states at half-integer band fillings in twisted bilayer graphene, Nat. Phys. **18**, 639 (2022).

[66] A. M. Läuchli, Z. Liu, E. J. Bergholtz, and R. Moessner, Hierarchy of Fractional Chern Insulators and Competing Compressible States, Phys. Rev. Lett. **111**, 126802 (2013).

[67] F. Cagliari, B. D. Fabio, and C. Landi, The natural pseudo-distance as a quotient pseudo-metric, and applications, Forum Mathematicum **27**, 1729 (2015).

[68] B. Mera and T. Ozawa, Kähler geometry and Chern insulators: Relations between topology and the quantum metric, Phys. Rev. B **104**, 045104 (2021).

[69] N. Howes, *Modern Analysis and Topology* (Springer, New York, 2012).

[70] See Supplemental Material at http://link.aps.org/supplemental/10.1103/PhysRevResearch.5.L012015 for details about the definition of the quantum metric, the projected interacting Hamiltonian and additional results regarding the hole dispersion.

[71] A. Abouelkomsan, Z. Liu, and E. J. Bergholtz, Particle-Hole Duality, Emergent Fermi Liquids, and Fractional Chern Insulators in Moiré Flatbands, Phys. Rev. Lett. **124**, 106803 (2020).

[72] B. L. Chittari, G. Chen, Y. Zhang, F. Wang, and J. Jung, Gate-Tunable Topological Flat Bands in Trilayer Graphene Boron-Nitride Moiré Superlattices, Phys. Rev. Lett. **122**, 016401 (2019).

[73] F. C. Zhang and S. Das Sarma, Excitation gap in the fractional quantum Hall effect: Finite layer thickness corrections, Phys. Rev. B **33**, 2903 (1986).

[74] Y.-H. Zhang, D. Mao, and T. Senthil, Twisted bilayer graphene aligned with hexagonal boron nitride: Anomalous Hall effect and a lattice model, Phys. Rev. Res. **1**, 033126 (2019).

[75] B. A. Bernevig and N. Regnault, Emergent many-body translational symmetries of Abelian and non-Abelian fractionally filled topological insulators, Phys. Rev. B **85**, 075128 (2012).

[76] Y. Cao, V. Fatemi, A. Demir, S. Fang, S. L. Tomarken, J. Y. Luo, J. D. Sanchez-Yamagishi, K. Watanabe, T. Taniguchi, E. Kaxiras, R. C. Ashoori, and P. Jarillo-Herrero, Correlated insulator behaviour at half-filling in magic-angle graphene superlattices, Nature (London) **556**, 80 (2018).

[77] Y. Cao, V. Fatemi, S. Fang, K. Watanabe, T. Taniguchi, E. Kaxiras, and P. Jarillo-Herrero, Unconventional superconductivity in magic-angle graphene superlattices, Nature (London) **556**, 43 (2018).

[78] G. Chen, L. Jiang, S. Wu, B. Lyu, H. Li, B. L. Chittari, K. Watanabe, T. Taniguchi, Z. Shi, J. Jung, Y. Zhang, and F. Wang, Evidence of a gate-tunable Mott insulator in a trilayer graphene Moiré superlattice, Nat. Phys. **15**, 237 (2019).

[79] G. Chen, A. L. Sharpe, P. Gallagher, I. T. Rosen, E. J. Fox, L. Jiang, B. Lyu, H. Li, K. Watanabe, T. Taniguchi, J. Jung, Z. Shi, D. Goldhaber-Gordon, Y. Zhang, and F. Wang, Signatures of tunable superconductivity in a trilayer graphene Moiré superlattice, Nature (London) **572**, 215 (2019).

[80] G. Chen, A. L. Sharpe, E. J. Fox, Y.-H. Zhang, S. Wang, L. Jiang, B. Lyu, H. Li, K. Watanabe, T. Taniguchi, Z. Shi, T. Senthil, D. Goldhaber-Gordon, Y. Zhang, and F. Wang, Tunable correlated Chern insulator and ferromagnetism in a Moiré superlattice, Nature (London) **579**, 56 (2020).

[81] G. Chen, A. L. Sharpe, E. J. Fox, S. Wang, B. Lyu, L. Jiang, H. Li, K. Watanabe, T. Taniguchi, M. F. Crommie, M. A. Kastner, Z. Shi, D. Goldhaber-Gordon, Y. Zhang, and F. Wang, Tunable orbital ferromagnetism at noninteger filling of a Moiré superlattice, Nano Lett. **22**, 238 (2022).

[82] Y. Choi, H. Kim, Y. Peng, A. Thomson, C. Lewandowski, R. Polski, Y. Zhang, H. S. Arora, K. Watanabe, T. Taniguchi, J. Alicea, and S. Nadj-Perge, Correlation-driven topological phases in magic-angle twisted bilayer graphene, Nature (London) **589**, 536 (2021).

[83] Y. Choi, H. Kim, C. Lewandowski, Y. Peng, A. Thomson, R. Polski, Y. Zhang, K. Watanabe, T. Taniguchi, J. Alicea, and S. Nadj-Perge, Interaction-driven band flattening and correlated phases in twisted bilayer graphene, Nat. Phys. **17**, 1375 (2021).

[84] J.-X. Lin, Y.-H. Zhang, E. Morissette, Z. Wang, S. Liu, D. Rhodes, K. Watanabe, T. Taniguchi, J. Hone, and J. I. A. Li, Spin-orbit– driven ferromagnetism at half Moiré filling in magic-angle twisted bilayer graphene, Science **375**, 437 (2022).

[85] X. Lu, P. Stepanov, W. Yang, M. Xie, M. A. Aamir, I. Das, C. Urgell, K. Watanabe, T. Taniguchi, G. Zhang, A. Bachtold, A. H. MacDonald, and D. K. Efetov, Superconductors, orbital magnets and correlated states in magic-angle bilayer graphene, Nature (London) **574**, 653 (2019).

[86] K. P. Nuckolls, M. Oh, D. Wong, B. Lian, K. Watanabe, T. Taniguchi, B. A. Bernevig, and A. Yazdani, Strongly correlated Chern insulators in magic-angle twisted bilayer graphene, Nature (London) **588**, 610 (2020).

[87] M. Oh, K. P. Nuckolls, D. Wong, R. L. Lee, X. Liu, K. Watanabe, T. Taniguchi, and A. Yazdani, Evidence for unconventional superconductivity in twisted bilayer graphene, Nature (London) **600**, 240 (2021).

[88] Y. Saito, J. Ge, L. Rademaker, K. Watanabe, T. Taniguchi, D. A. Abanin, and A. F. Young, Hofstadter subband ferromagnetism and symmetry-broken Chern insulators in twisted bilayer graphene, Nat. Phys. **17**, 478 (2021).

[89] A. L. Sharpe, E. J. Fox, A. W. Barnard, J. Finney, K. Watanabe, T. Taniguchi, M. A. Kastner, and D. Goldhaber-Gordon, Emergent ferromagnetism near three-quarters filling in twisted bilayer graphene, Science **365**, 605 (2019).

[90] A. L. Sharpe, E. J. Fox, A. W. Barnard, J. Finney, K. Watanabe, T. Taniguchi, M. A. Kastner, and D. Goldhaber-Gordon, Evidence of orbital ferromagnetism in twisted bilayer graphene aligned to hexagonal boron nitride, Nano Lett. **21**, 4299 (2021).

[91] C.-C. Tseng, X. Ma, Z. Liu, K. Watanabe, T. Taniguchi, J.-H. Chu, and M. Yankowitz, Anomalous Hall effect at half filling in twisted bilayer graphene, Nat. Phys. **18**, 1038 (2022).

[92] S. Wu, Z. Zhang, K. Watanabe, T. Taniguchi, and E. Y. Andrei, Chern insulators, van Hove singularities and topological flat bands in magic-angle twisted bilayer graphene, Nat. Mater. **20**, 488 (2021).

[93] Y. Xie, B. Lian, B. Jäck, X. Liu, C.-L. Chiu, K. Watanabe, T. Taniguchi, B. A. Bernevig, and A. Yazdani, Spectroscopic signatures of many-body correlations in magic-angle twisted bilayer graphene, Nature (London) **572**, 101 (2019).

[94] M. Yankowitz, S. Chen, H. Polshyn, Y. Zhang, K. Watanabe, T. Taniguchi, D. Graf, A. F. Young, and C. R. Dean, Tuning superconductivity in twisted bilayer graphene, Science **363**, 1059 (2019).

[95] H. Zhou, T. Xie, A. Ghazaryan, T. Holder, J. R. Ehrets, E. M. Spanton, T. Taniguchi, K. Watanabe, E. Berg, M. Serbyn, and A. F. Young, Half- and quarter-metals in rhombohedral trilayer graphene, Nature (London) **598**, 429 (2021).

[96] Y.-H. Zhang, D. Mao, Y. Cao, P. Jarillo-Herrero, and T. Senthil, Nearly flat Chern bands in Moiré superlattices, Phys. Rev. B **99**, 075127 (2019).

[97] D. A. G. González, B. L. Chittari, Y. Park, J.-H. Sun, and J. Jung, Topological phases in N-layer ABC graphene/boron nitride Moiré superlattices, Phys. Rev. B **103**, 165112 (2021).

[98] Y.-H. Zhang and T. Senthil, Bridging Hubbard model physics and quantum Hall physics in trilayer graphene/HBN Moiré superlattice, Phys. Rev. B **99**, 205150 (2019).

[99] C. Repellin and T. Senthil, Chern bands of twisted bilayer graphene: Fractional Chern insulators and spin phase transition, Phys. Rev. Res. **2**, 023238 (2020).

[100] P. Wilhelm, T. C. Lang, and A. M. Läuchli, Interplay of fractional Chern insulator and charge density wave phases in twisted bilayer graphene, Phys. Rev. B **103**, 125406 (2021).

[101] D. Bauer, S. Talkington, F. Harper, B. Andrews, and R. Roy, Fractional Chern insulators with a non-Landau level continuum limit, Phys. Rev. B **105**, 045144 (2022).